

# Dynamical Ordering and Directional Locking For Particles Moving Over Quasicrystalline Substrates

C. Reichhardt and C. J. Olson Reichhardt

*Theoretical Division, Los Alamos National Laboratory, Los Alamos, New Mexico 87545, USA*

(Dated: October 18, 2018)

We use molecular dynamics simulations to study the driven phases of particles such as vortices or colloids moving over a decagonal quasiperiodic substrate. In the regime where the pinned states have quasicrystalline ordering, the driven phases can order into moving square or smectic states, or into states with aligned rows of both square and triangular tiling which we term dynamically induced Archimedean-like tiling. We show that when the angle of the drive is varied with respect to the substrate, directional locking effects occur where the particle motion locks to certain angles. It is at these locking angles that the dynamically induced Archimedean tiling appears. We also demonstrate that the different dynamical orderings and locking phases show pronounced changes as a function of filling fraction.

PACS numbers: 05.60.Cd, 74.25.Wx, 05.45.-a, 82.70.Dd

Quasicrystals have received intense study since their discovery due to their unusual property of combining nonperiodicity with long-range order [1]. Recently there has been growing interest in understanding how interacting particles such as vortices in type-II superconductors [2–4] or charged colloidal particles [5–9] order in the presence of a quasicrystalline substrate created with nanolithographic or optical techniques. On a fully periodic substrate, these types of particles form states that are commensurate with the periodicity of the substrate at fillings which meet integer or fractional matching conditions [10–13]. In the case of vortices, the commensurate fillings are associated with peaks in the critical current or the external force required to depin the vortices from the substrate [10, 11]. When vortices interact with quasicrystalline Penrose or decagonal pinning site arrays, a new set of peaks in the critical current appear at non-rational fields in addition to the commensurate fields due to a novel type of ordering of the vortices on these substrates [2, 3]. For colloids interacting with decagonal substrates, experiments show that strong substrates produce quasicrystalline order of the colloids but weak substrates permit the triangular lattice favored by the colloid-colloid interactions to form. Remarkably, for intermediate substrate strengths a new type of ordering arises consisting of a combination of triangular and square order. This has been termed an Archimedean-like tiling [5, 8].

Numerous experimental and simulation studies have been performed on the dynamic phases of a collection of particles driven over a periodic substrate. One of the most striking observations is directional locking in which the particles cease to follow the direction of the drive and instead lock to a symmetry direction of the substrate. The locking effect produces a series of pronounced steps in the velocity versus drive angle curve [14, 15]. Directional locking effects were experimentally observed for colloids moving through a periodic optical trap array [16, 17] and for vortices driven at differing an-

gles with respect to a pinning substrate [18]. For colloidal systems, directional locking can be used for practical applications such as the fractionation of different species of particles, only one of which locks to the symmetry direction of the substrate [17, 19]. An open question is whether directional locking can also occur for particles moving over quasiperiodic substrates. It has already been shown that the nonequilibrium, driven state for particles driven over random substrates can show dynamically induced ordered states which are inaccessible to the static system. For example, on strong random substrates which produce a disordered pinned state, the driven state can partially order to a moving smectic or to a triangular lattice [20, 21].

Here we show that directional locking and dynamical ordering can occur for particles moving over quasicrystalline substrates. The dynamical ordering occurs only for certain driving directions, and changes the system from a quasicrystalline pinned state to a moving state with novel dynamical ordering that is similar to a square and triangular tiling. We call this ordering a dynamically induced Archimedean tiling. Other types of ordering to moving smectic, moving square, and moving liquid states are also possible as a function of filling and drive direction. We specifically demonstrate the locking and ordering for vortices in type-II superconductors, and note that the same results appear for charged colloids moving over decagonal substrates [22].

We model a two-dimensional system of  $N_v$  interacting particles in the presence of a pinning array with 5-fold Penrose ordering, as shown in Fig. 1(a). In the superconducting system we consider a sample of size  $24\lambda \times 24\lambda$  with periodic boundary conditions, where  $\lambda$  is the London penetration depth. The vortex motion evolves according to the following overdamped equation:  $\eta \frac{d\mathbf{R}_i}{dt} = \mathbf{F}_i^{vv} + \mathbf{F}_i^p + \mathbf{F}_i^{ext}$ . Here  $\mathbf{R}_i$  is the location of vortex  $i$  and  $\eta$  is the damping coefficient. The repulsive vortex-vortex interaction force is  $\mathbf{F}_i^{vv} =$

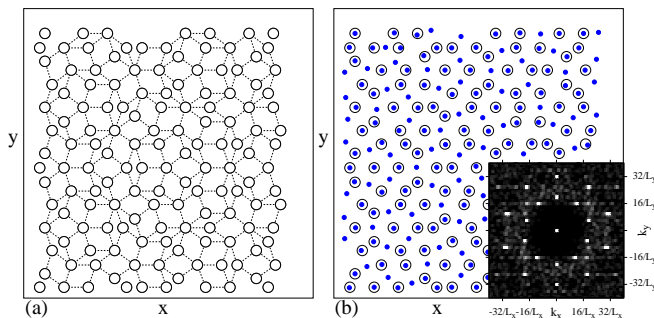


FIG. 1: (a) The locations of the Penrose tiled pinning sites (open circles) for a portion of the sample. Dashed lines indicate the positions of the Penrose tiles used to define the pinning locations. (b) The location of the vortices (filled circles) and pinning sites (open circles) at  $B/B_\phi = 1.61$  in the same sample at zero applied drive. Here  $B_\phi$  is the field at which the number of vortices equals the number of pinning sites. Inset: The structure factor  $S(k)$  of the vortex positions from (b) has tenfold peaks indicative of quasicrystalline order.

$\sum_{j \neq i}^{N_v} f_0 K_1(R_{ij}/\lambda) \hat{\mathbf{R}}_{ij}$ , where  $K_1$  is the modified Bessel function,  $f_0 = \phi_0^2 / (2\pi\mu_0\lambda^3)$ ,  $\phi_0 = h/2e$  is the elementary flux quantum,  $R_{ij} = |\mathbf{R}_i - \mathbf{R}_j|$ , and  $\hat{\mathbf{R}} = (\mathbf{R}_i - \mathbf{R}_j)/R_{ij}$ . The substrate force from  $N_p$  parabolic traps of radius  $r_p = 0.35\lambda$  and maximum strength  $F_p = 1.85$  has the form  $\mathbf{F}_i^{vv} = \sum_{k=0}^{N_p} f_0 (F_p/r_p) \Theta(1 - R_{ik}/R_p) \hat{\mathbf{R}}_{ik}$ , where  $\Theta$  is the Heaviside step function. At the matching field of  $B_\phi$ ,  $N_v/N_p = 1$ .  $\mathbf{F}_i^{ext}$  is the driving force from an external current applied uniformly to all particles. We initialize the particle positions using simulated annealing, then slowly turn on an external drive  $\mathbf{F}^{ext} = F_D(\cos\theta\hat{\mathbf{x}} + \sin\theta\hat{\mathbf{y}})$  with  $\theta$  reported in degrees. We measure the velocity in the  $y$ -direction  $V_y = \sum_{i=0}^{N_v} \mathbf{v}_i \cdot \hat{\mathbf{y}}$  as we increment the drive angle  $\theta$ . All forces and lengths are measured in units of  $f_0$  and  $\lambda$ .

In Fig. 1(a) we plot the pinning site locations showing the 5-fold Penrose tiling and in Fig. 1(b) we show the positions of the non-driven pinned particle state at  $B/B_\phi = 1.61$ . The structure factor  $S(k)$  of the particle positions in this sample plotted in the inset of Fig. 1(d) has a 10-fold peak structure, indicative of quasicrystalline order such as that found in the strong substrate limit for colloidal systems [5]. In general, for this  $F_p$  the pinned states at different filling fractions have quasicrystalline ordering.

Figure 2(a) shows  $\langle V_y \rangle$  versus the drive angle  $\theta$  for a sample with  $B/B_\phi = 3.225$  and  $F_D = 2.0$ . At this drive, all the particles are in motion. The clear set of steps in  $\langle V_y \rangle$  is a signature of the directional locking that occurs when the particles move along a single direction over a range of drive angles [14–17, 19]. For the same set of parameters but with randomly placed pinning, no steps occur in  $\langle V_y \rangle$  [22]. The locking angles are related to the tenfold orientational ordering, and occur at multiples of

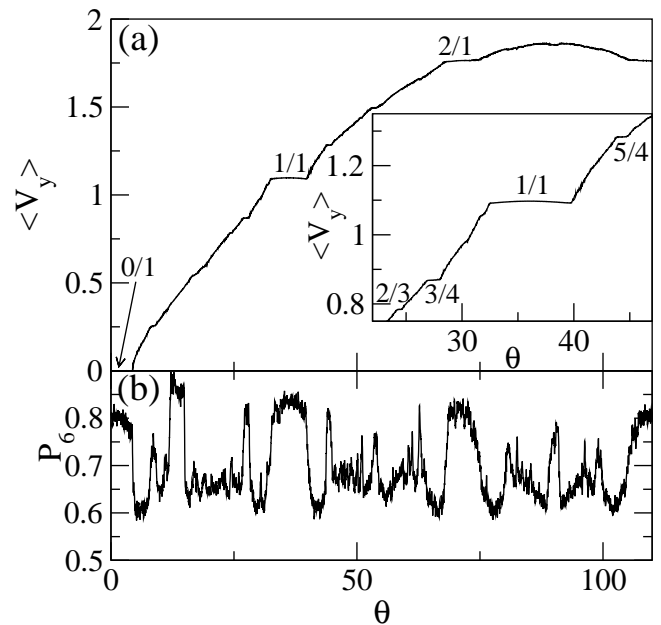


FIG. 2: (a) The average velocity in the  $y$ -direction  $\langle V_y \rangle$  vs drive angle  $\theta$  for the system in Fig. 1(a) with  $B/B_\phi = 3.225$  at  $F_D = 2.0$ . A series of pronounced steps appear at multiples of  $36^\circ$ , marked 0/1, 1/1, and 2/1, when the particle motion becomes locked to certain symmetry directions of the substrate. Locking at fractional multiples of  $36^\circ$  produces many smaller steps. Inset: A blow up of the main panel near the 1/1 step showing some of the fractional steps. (b) The corresponding  $P_6$  vs  $\theta$  showing that the system is more ordered on the locking steps.

$\theta = 360^\circ/10 = 36^\circ$ , as highlighted in Fig. 2(a) for  $\theta = 0^\circ$  (the 0/1 step),  $36^\circ$  (the 1/1 step), and  $72^\circ$  (the 2/1 step). There are numerous smaller locking steps associated with rational fractions of  $36^\circ$ , including  $1/4$ ,  $1/2$ ,  $2/3$ ,  $3/4$ ,  $5/4$ , and  $5/2$ . Some of these smaller steps are visible in the inset of Fig. 2(a), which shows a blowup of the main panel. This result proves that it is possible for directional locking to occur on quasiperiodic substrates, indicating that *orientational order* rather than translational order of the substrate is the essential ingredient for directional locking. This opens the possibility of creating novel fractionation devices using quasiperiodic substrates, and may also be relevant to understanding frictional studies performed with quasicrystalline substrates. We find that on the locking steps, there is a higher amount of order in the particle lattice. In Fig. 2(b) we plot the fraction of sixfold coordinated particles  $P_6 = \sum_i^{N_v} \delta(z_i - 6)$  as a function of  $\theta$ , where the particle coordination number  $z_i$  is obtained from a Voronoi construction that is not sensitive to square orderings. In the pinned state  $P_6 = 0.525$ , while for the driven systems  $P_6$  reaches its highest values on the locking steps and is lower in the non-locking ranges of  $\theta$ .

We tessellate the positions of the particles in the mov-

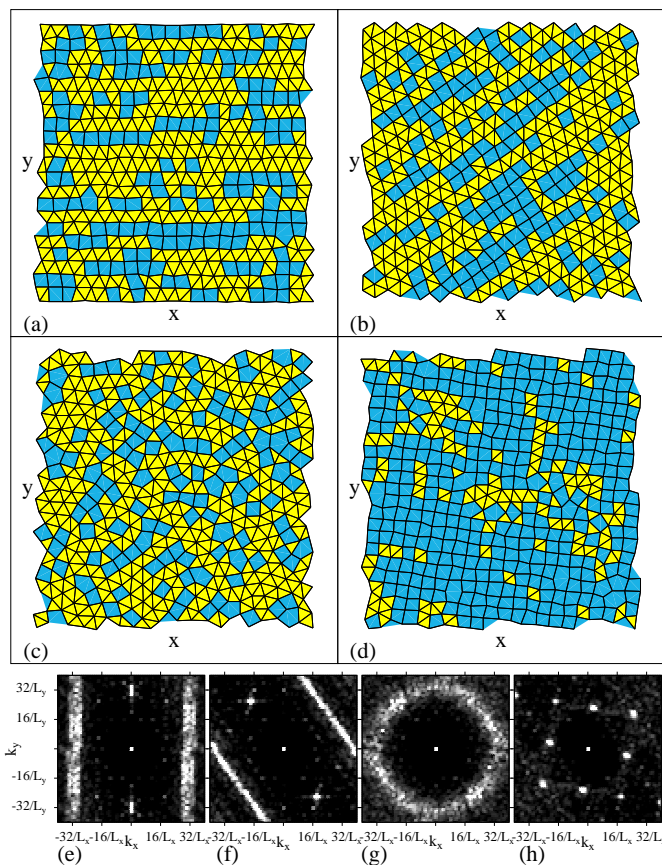


FIG. 3: Delaunay triangulations of the particle positions in the sliding state. Bonds longer than  $1.1a_0$  are omitted, where  $a_0$  is the lattice spacing of a triangular lattice with the same density. Yellow (light) polygons are triangular and blue (dark) polygons are square or nontriangular. For a sample with  $B/B_\phi = 3.225$  and  $F_D = 2.0$  we show (a) the 0/1 step at  $\theta = 0$  exhibiting the oriented triangles and squares of the dynamically induced Archimedean tiling, (b) the 1/1 step at  $\theta = 32^\circ$  where the Archimedean ordering aligns with the direction of motion, and (c)  $\theta = 41^\circ$  in the unlocked region just above the 1/1 step. (d) The triangulation for the 1/1 step at  $\theta = 32^\circ$  for a sample with  $B/B_\phi = 1.61$  and  $F_D = 2.0$ , where most of the tiles are square. Smectic-like ordering appears in  $S(k)$  corresponding to the Archimedean tilings of (e) panel (a) and (f) panel (b). (g)  $S(k)$  for the unlocked state shown in panel (c) has a ring structure indicating liquid ordering. (h) At the lower field of  $B/B_\phi = 1.61$ ,  $S(k)$  corresponding to panel (d) has square ordering.

ing state as in Refs. [5, 8] in order to reveal the nature of the dynamical ordering. In Fig. 3(a) we show the tessellation of the moving state on the 0/1 step from Fig. 2(a), where the flow is locked in the  $x$ -direction. Both square and triangular tiles are present, and the square tiles are aligned with the flow along the  $x$  direction. This state is very similar to the Archimedean type tiling found for colloids pinned by substrates of intermediate strength [5, 8]. The smectic features of the corresponding structure factor  $S(k)$  in Fig. 3(e) indicate that unlike the static col-

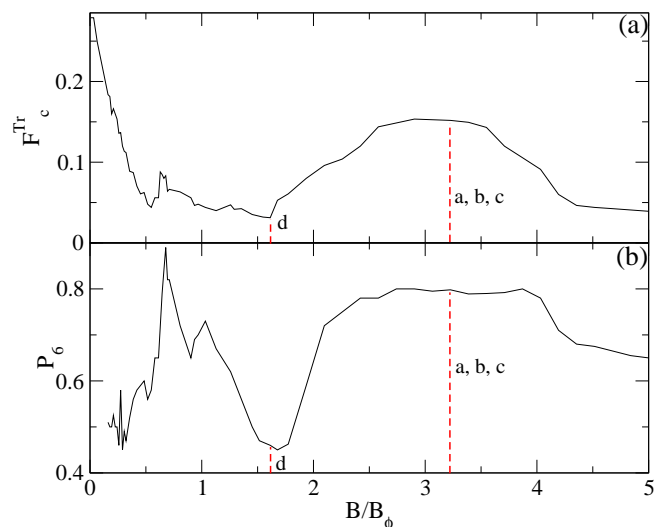


FIG. 4: (a) The depinning threshold  $F_c^{Tr}$  indicating the width of the 0/1 locking step vs  $B/B_\phi$ . (b)  $P_6$  vs  $B/B_\phi$ . The broad peak in both quantities for  $1.7 < B/B_\phi < 4.3$  appears when the system forms the dynamical Archimedean tiling illustrated in Fig. 3(a), while the dip at  $B/B_\phi = 1.6$  corresponds to the moving square structure shown in Fig. 3(h). Additional peaks in  $P_6$  occur at  $B/B_\phi = 1.0$  and  $B/B_\phi = 1/\tau$ , where  $\tau$  is the golden mean. Dashed lines and the labels a-d indicate the fields shown in Fig. 3(a-d).

loidal tiling, the dynamical tiling does not have a one-dimensional (1D) quasiperiodic structure, which would appear as a series of peaks in  $S(k)$  [8]. More recent colloid experiments reveal the development of smeared smectic-like peaks in  $S(k)$  similar to those in Fig. 3(e) when the strength of the laser-induced substrate is increased [9]. Moving smectic states also appear in systems with random pinning, but these states have a purely triangular tiling containing some dislocations [20, 21].

We find that oriented Archimedean tilings appear on each locking step, as illustrated for the 1/1 step in Fig. 3(b) and (f). The particles move along 1D channels on the locked steps [22], but follow winding and rapidly changing trajectories when not on the steps. In Fig. 3(c) we show the tessellation for driving just above the 1/1 step in a disordered flow regime. The orientational ordering is lost and the corresponding  $S(k)$  in Fig. 3(g) has a ring structure characteristic of a moving liquid [20]. We find that the relative number of square and rectangular tiles appearing on the locking steps varies as a function of filling. For example, at  $B/B_\phi = 1.61$  on the 1/1 locking step, Fig. 3(d) shows that the tiling is predominantly square, and  $S(k)$  in Fig. 3(h) has square ordering.

To understand where the different moving phases occur as well as the changes in the effectiveness of the directional locking, in Fig. 4(a) we plot the transverse depinning force  $F_c^{Tr}$  determined by  $F_c^{Tr} = F_D \sin \theta_e$ , where  $\theta_e$  is the end of the 0/1 locking step, versus  $B/B_\phi$  and

in Fig. 4(b) we show the corresponding  $P_6$  versus  $B/B_\phi$ . There is a broad maximum in  $F_c^{Tr}$  associated with the Archimedean type ordering for  $1.7 < B/B_\phi < 4.3$  and another sharper peak in  $F_c^{Tr}$  at  $B/B_\phi = 0.62$ . Both of these features are accompanied by peaks in  $P_6$ . Our transverse depinning measurements, in which the vortices are depinning from a moving state, differ in several ways from the longitudinal depinning from a static state previously measured in simulations and experiments [2, 3, 23]. For example,  $F_c^{Tr}$  shows no peaks at  $B/B_\phi = 0.81$  or  $1.0$ , although we do find a weak peak in  $P_6$  at  $B/B_\phi = 1.0$ . In agreement with the experiment of Ref. [3], we observe a prominent peak in  $F_c^{Tr}$  at  $B/B_\phi = 0.62 = 1/\tau$  where  $\tau = (1 + \sqrt{5})/2$  is the golden mean. The lowest value of  $F_c^{Tr}$  occurs at  $B/B_\phi = 1.61 \approx \tau$ . At this field, the widths of the locking steps are suppressed and the system has the square ordering shown in Fig. 3(d,h). For  $B/B_\phi > 4.0$ , the ordering of the locked phases is reduced and  $S(k)$  develops a ring structure on the locking steps, while the vortex-vortex interactions are strong enough in the nonlocking regimes to produce sixfold ordering. For  $0.5 < B/B_\phi < 1.5$  the system generally exhibits a smectic ordering containing few square tiles corresponding to a highly defected triangular lattice similar to that found for driving over random substrates.

We find that the ordered moving phases only occur when  $F_D$  is sufficiently large. For  $F_D < 1.25$  with  $F_p = 1.85$ , significant plastic flow occurs,  $S(k)$  is always liquidlike, and the step structures in the velocity curves disappear. For  $F_D \gg F_p$  the width of the steps slowly decreases with increasing  $F_D$ . We also find the same results reported here for driven colloids interacting with a screened Coulomb interaction and a quasiperiodic substrate [22]. Sevenfold or tetradecagonal quasiperiodic substrates also produce directional locking, but the locking steps are significantly reduced in width [22].

We have shown that interacting particles such as vortices or colloids driven over a quasiperiodic substrate exhibit rich dynamical behaviors including pronounced directional locking where the particles prefer to move at particular angles with respect to the substrate. Directional locking has already been studied in periodic systems, but this study is the first demonstration of directional locking on quasiperiodic substrates. For strong substrates, the pinned state has quasicrystalline ordering, but the moving state can have square or smectic ordering depending on the orientation of the drive. At certain filling fractions the system forms a moving Archimedean tiling ordered state similar to the pinned Archimedean tiling ordering observed for colloids on decagonal substrates, but with smectic rather than quasiperiodic character. We also show that the dynamically ordered states produce distinct signatures in the transverse depinning threshold.

This work was carried out under the auspices of the NNSA of the U.S. DoE at LANL under Contract No.

DE-AC52-06NA25396.

- 
- [1] D. Shechtman, I. Blech, D. Gratias, and J.W. Cahn, Phys. Rev. Lett **53**, 1951 (1984); J.-B. Suck, M. Schreiber, and P. Häussler, Eds., *Quasicrystals* (Springer-Verlag, Berlin, 2002).
  - [2] V. Misko, S. Savel'ev, and F. Nori, Phys. Rev. Lett. **95**, 177007 (2005); Phys. Rev. B **74**, 024522 (2006); M. Kemmler *et al.*, Phys. Rev. Lett. **97**, 147003 (2006).
  - [3] A.V. Silhanek *et al.*, Appl. Phys. Lett. **89**, 152507 (2006).
  - [4] J.E. Villegas, M.I. Montero, C.-P. Li, and I.K. Schuller, Phys. Rev. Lett. **97**, 027002 (2006).
  - [5] J. Mikhael, J. Roth, L. Helden, and C. Bechinger, Nature (London) **454**, 501 (2008).
  - [6] M. Schmiedeberg and H. Stark, Phys. Rev. Lett. **101**, 218302 (2008).
  - [7] J. Mikhael *et al.*, Proc. Nat. Acad. Sci. (USA) **107**, 7214 (2010).
  - [8] M. Schmiedeberg *et al.*, Eur. Phys. J. E **32**, 25 (2010).
  - [9] J. Mikhael, G. Gera, T. Bohlein, and C. Bechinger, Soft Matter, in press (2010).
  - [10] M. Baert *et al.*, Phys. Rev. Lett. **74**, 3269 (1995); J.I. Martín *et al.*, *ibid.* **79**, 1929 (1997).
  - [11] C. Reichhardt, C.J. Olson, and F. Nori, Phys. Rev. B **57**, 7937 (1998).
  - [12] K. Harada *et al.*, Science **274**, 1167 (1996); G. Karapetrov *et al.*, Phys. Rev. Lett. **95**, 167002 (2005).
  - [13] C. Reichhardt and C.J. Olson, Phys. Rev. Lett. **88**, 248301 (2002); M. Brunner and C. Bechinger, *ibid.* **88**, 248302 (2002); A. Sarlah, E. Frey, and T. Franosch, Phys. Rev. E **75**, 021402 (2007); S. El Shawish, J. Dobnikar, and E. Trizac, Soft Matter **4**, 1491 (2008).
  - [14] C. Reichhardt and F. Nori, Phys. Rev. Lett. **82**, 414 (1999).
  - [15] J. Wiersig and K.-H. Ahn, Phys. Rev. Lett. **87**, 026803 (2001).
  - [16] P.T. Korda, M.B. Taylor, and D.G. Grier, Phys. Rev. Lett. **89**, 128301 (2002).
  - [17] M.P. MacDonald, G.C. Spalding, and K. Dholakia, Nature (London) **426**, 421 (2003); A.M. Lacasta, J.M. Sancho, A.H. Romero, and K. Lindenberg, Phys. Rev. Lett. **94**, 160601 (2005); B.R. Long *et al.*, Phys. Rev. E **78**, 046304 (2008); K. Xiao and D.G. Grier, Phys. Rev. Lett. **104**, 028302 (2010).
  - [18] R. Surdeanu *et al.*, Europhys. Lett. **54**, 682 (2001); A.V. Silhanek *et al.*, Phys. Rev. B **68**, 214504 (2003); J.E. Villegas *et al.*, *ibid.* **68**, 224504 (2003).
  - [19] M. Balvin *et al.*, Phys. Rev. Lett. **103**, 078301 (2009); J. Koplik and G. Drazer, Phys. Fluids **22**, 052005 (2010).
  - [20] A.E. Koshelev and V.M. Vinokur, Phys. Rev. Lett. **73**, 3580 (1994); K. Moon, R.T. Scalettar, and G.T. Zimányi, Phys. Rev. Lett. **77**, 2778 (1996); C.J. Olson, C. Reichhardt, and F. Nori, *ibid.*, **81**, 3757 (1998); F. Pardo *et al.*, Nature (London) **396**, 348 (1998).
  - [21] P. Le Doussal and T. Giamarchi, Phys. Rev. B **57**, 11356 (1998); L. Balents, M.C. Marchetti, and L. Radzihovsky, Phys. Rev. B **57**, 7705 (1998).
  - [22] See EPAPS Document No. xx.
  - [23] R.B.G. Kramer *et al.*, Phys. Rev. Lett. **103**, 067007 (2009).

SUPPLEMENTARY MATERIAL

**Directional Locking for Vortices on Tetradeagonal Quasicrystalline Substrates**

Here, we show that the directional locking effects described in the main text for driven vortices moving over decagonal quasicrystalline substrates also occur when the vortices are driven over tetradeagonal or sevenfold-symmetric quasicrystalline substrates such as that shown in Suppl. Fig. 1. We use the same pinning parameters as for the decagonal substrate with  $F_p = 1.85$  and  $r_p = 0.35\lambda$ , and apply a drive  $F_D = 2.0$  at  $B/B_\phi = 3.9$ . In Suppl. Fig. 2(a) we plot  $\langle V_y \rangle$  versus the drive angle  $\theta$  and in Suppl. Fig. 2(b) we show the fraction of sixfold coordinated particles  $P_6$  versus  $\theta$ . There is a clear set of steps in  $\langle V_y \rangle$  which are accompanied by enhanced sixfold ordering as shown by the increases in  $P_6$ . For the tetradeagonal substrate potential, the major locking steps occur at drive angles that are integer multiples of  $360^\circ/14$ , producing the 1/1 step at  $25.7^\circ$ , the 2/1 step at  $51.42^\circ$ , and the 3/1 step at  $77^\circ$ . For the decagonal substrate the locking steps fall at integer multiples of  $360^\circ/10$ , as described in the main text. Fractional locking steps are nearly absent for the tetradeagonal substrate; however, for lower fillings it is possible to resolve some fractional steps. This is shown in Suppl. Fig. 3(a,b) for  $B/B_\phi = 2.96$ . The fractional steps  $m/4$  with  $m$  integer are the most pronounced and are associated with enhanced sixfold ordering in  $P_6$ . This result indicates that directional locking is a generic feature for particles moving over different types of quasicrystalline substrates. The width of the locking steps is generally much narrower for the tetradeagonal substrate than for the decagonal substrate. Additionally, although the decagonal substrate produced pronounced five-fold ordering of the particles for some fillings, we do not find strong sevenfold particle ordering on the tetradeagonal substrate. Instead, on the locking steps, we observe smectic ordering composed of sixfold-coordinated particles and a limited number of dislocations.

**Directional Locking for Colloids on Decagonal and Tetradeagonal Substrates**

We next show that the same directional locking effects described in the main text for vortices driven over quasicrystalline substrates also occurs for colloidal particles driven over quasicrystalline substrates. We model a two-dimensional system of  $N_c$  interacting colloids in the presence of fivefold and sevenfold quasicrystalline substrates. The substrate is composed of localized pinning traps with maximum strength  $F_p$  and radius  $r_p = 0.35$ . We simulate

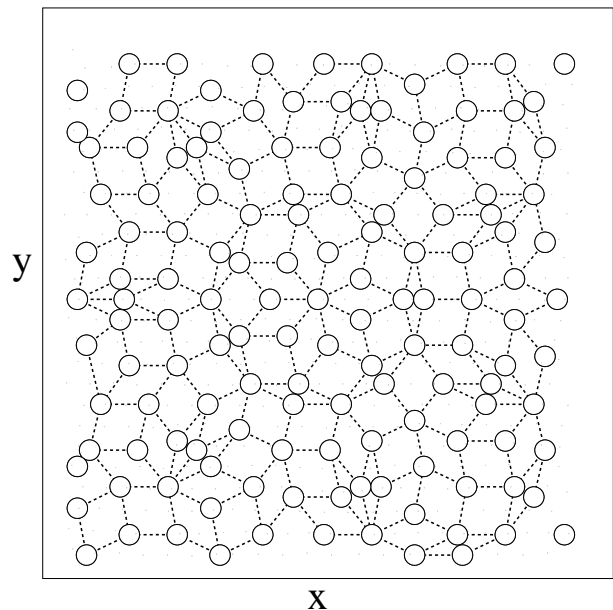


FIG. 1: The locations of the pinning sites (open circles) for a portion of the sample with seven-fold or tetradeagonal ordering. Dashed lines indicate the positions of the tiles used to define the pinning locations.

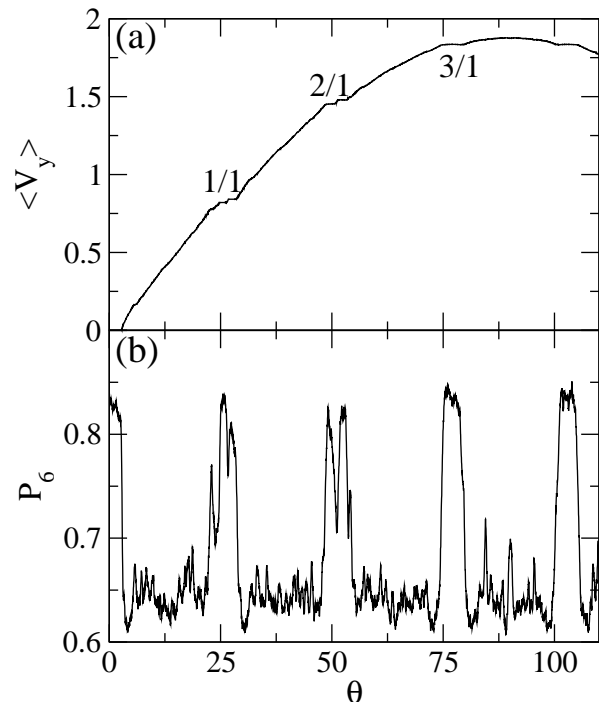


FIG. 2: (a) The average velocity in the  $y$ -direction  $\langle V_y \rangle$  vs drive angle  $\theta$  for the system in Suppl. Fig. 1 with a sevenfold quasicrystalline pinning array for  $F_p = 1.85$ ,  $r_p = 0.35\lambda$ ,  $B/B_\phi = 3.9$ , and  $F_D = 0.2$ . Several steps appear at the directional locking angles which are integer multiples of  $360^\circ/14$ . The 1/1, 2/1, 3/1, and 4/1 lockings are clearly visible. (b) The corresponding  $P_6$  vs  $\theta$  shows that on the locking steps the system develops a considerable amount of sixfold ordering.



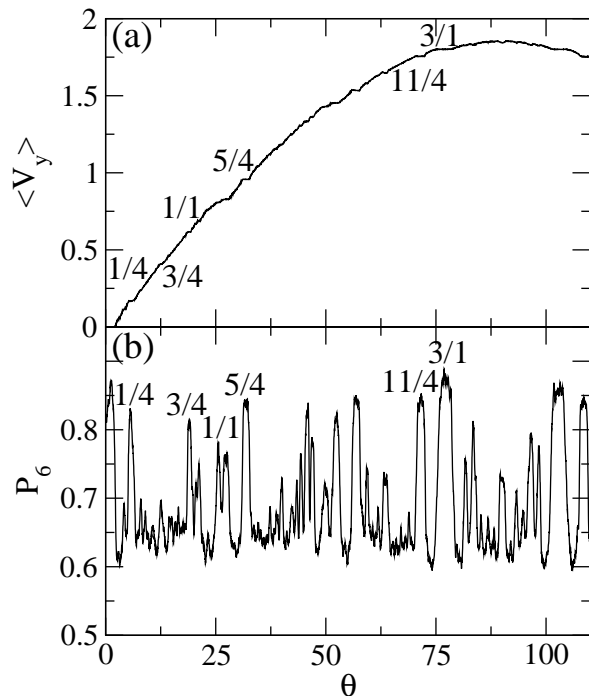


FIG. 3: (a)  $\langle V_y \rangle$  vs drive angle  $\theta$  for the system in Suppl. Fig. 2 but for a filling of  $B/B_\phi = 2.96$  where additional fractional locking steps are visible, particularly at fractions of  $m/4$  where  $m$  is an integer. Some representative steps are marked. (b) The corresponding  $P_6$  vs  $\theta$ .

the motion of the colloids using the same procedure used previously to model colloid dynamics on random substrates [1] and periodic substrates [2], by integrating the following equation of motion:  $\eta d\mathbf{R}_i/dt = \mathbf{F}_i^{cc} + \mathbf{F}_i^s + \mathbf{F}_D$ . Here  $\mathbf{R}_i$  is the location of colloid  $i$  and  $\eta$  is the damping coefficient. The colloid-colloid interaction potential has the Yukawa form  $V(R_{ij}) = (E_0/R_{ij})\exp(-\kappa R_{ij})$ , where  $R_{ij} = |\mathbf{R}_i - \mathbf{R}_j|$ ,  $E_0 = Z^{*2}/(4\pi\epsilon\epsilon_0)$ ,  $\epsilon$  is the solvent dielectric constant,  $Z^*$  is the effective charge of each colloid, and  $1/\kappa$  is the screening length. The colloid-colloid interactions are repulsive and are given by  $\mathbf{F}_i^{cc} = -\sum_{j \neq i}^{N_c} \nabla V(R_{ij})$ . Lengths are measured in units of  $a_0$  and forces in units of  $F_0 = E_0/a_0$ . The substrate force term  $\mathbf{F}_i^s$  comes from  $N_p$  pinning sites placed in a decagonal or tetradecagonal pattern and has the same form as described for the vortex system. The colloid density relative to the pinning density is  $N_c/N_p$ . We neglect hydrodynamic interactions in the colloidal system and assume that the colloids are in the low volume fraction, highly charged, electrophoretically driven limit. The external force  $\mathbf{F}_D$  is the same as that used for the vortex case and we measure  $\langle V_y \rangle$  and  $P_6$  as a function of the drive angle  $\theta$ .

In Suppl. Fig. 4(a) we plot  $\langle V_y \rangle$  versus  $\theta$  for a colloidal system on a decagonal substrate with  $F_p = 0.75$  at  $N_c/N_p = 2.9$ , and in Fig. 4(b) we show the corre-

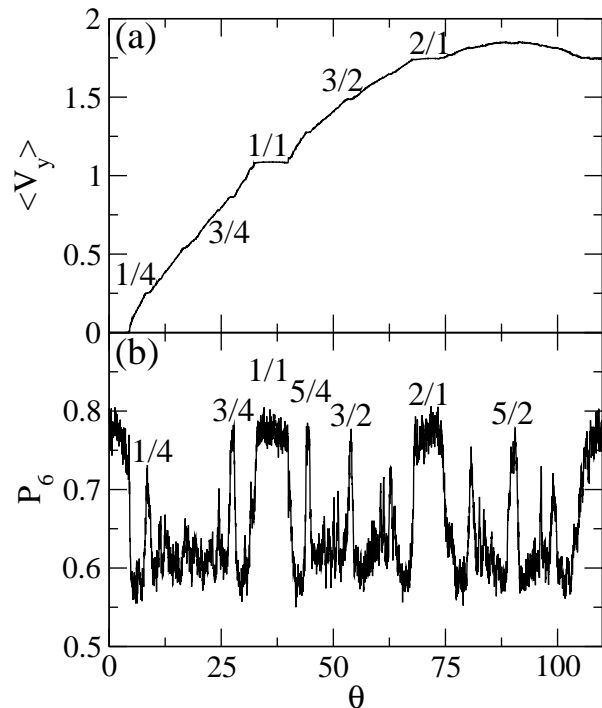


FIG. 4: The directional locking for charged colloidal particles driven over a decagonal substrate in the same manner as the vortices in the main text. Here  $N_c/N_p = 2.9$  and  $F_p = 0.75$ . In general, the same features observed for the vortex system also appear for the colloidal system. (a)  $\langle V_y \rangle$  vs  $\theta$  with the main locking steps at integer multiples of  $360^\circ/10$  highlighted at  $1/1$  and  $2/1$ . Several fractional steps also appear at rational fractions of the integer steps such as at  $1/4$ ,  $3/4$ , and  $3/2$ . (b) The corresponding  $P_6$  vs  $\theta$  shows that along the steps the system has higher ordering. On the main integer matching steps, the system forms the dynamically induced Archimedean ordering also observed in the vortex system (as described in the main text).

sponding  $P_6$  versus  $\theta$ . Here, all the general features of the directional locking in the vortex system also appear for the colloidal system, including the dominant locking steps at integer multiples of  $360^\circ/10$  such as  $1/1$  and  $2/1$  and additional fractional lockings at  $1/2$ ,  $3/2$ ,  $5/2$ ,  $1/4$ , and  $3/4$ . Each locking step is associated with enhanced ordering of the colloidal lattice when the system forms a dynamically ordered Archimedean tiling state.

In Suppl. Fig. 5(a,b) we show  $\langle V_y \rangle$  and  $P_6$  versus  $\theta$  for colloids moving over a tetradecagonal substrate. We find the same features illustrated in Suppl. Fig. 3 for vortices moving over a tetradecagonal substrate. The dominant locking steps occur at integer multiples of  $360^\circ/14$ . In general, the locking steps are weaker than for the decagonal substrate and the dominant fractional steps occur at ratios of  $m/4$  with  $m$  integer. The fractional steps are also associated with a series of peaks in  $P_6$ , where additional fractions beyond  $m/4$  appear as smaller peaks that

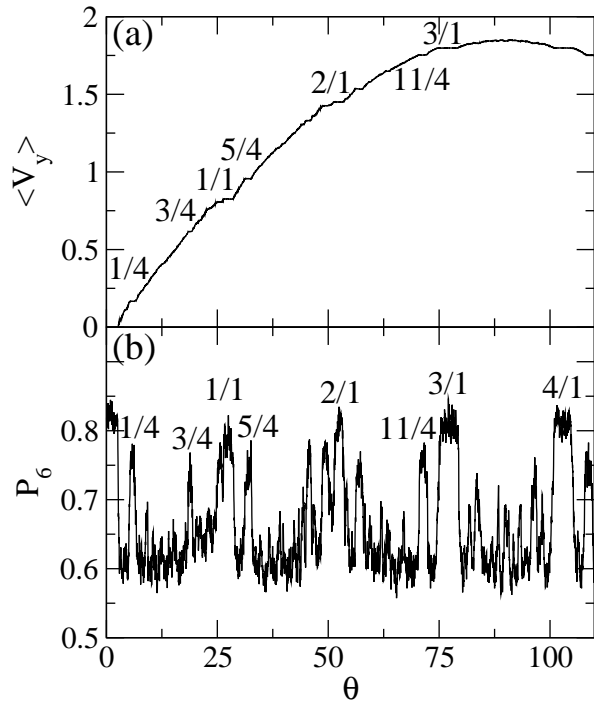


FIG. 5: Directional locking for charged colloidal particles driven over a sevenfold or tetradecagonal substrate for the same parameters in Suppl. Fig. 4. (a)  $\langle V_y \rangle$  vs  $\theta$  and (b)  $P_6$  vs  $\theta$ . The same features found for the vortex system in Suppl. Fig. 3 appear for the colloid system, including locking steps falling at integer multiples of  $360^\circ/14$ . We also observe the strongest fractional locking steps at fractions  $m/4$  with  $m$  integer.

do not show full ordering. These results indicate that the directional locking effects on quasicrystalline periodic substrates can be observed for various types of interacting particles including colloids and vortices, and that the directional locking is a robust feature in these systems.

- 
- [1] C. Reichhardt and C.J. Olson, Phys. Rev. Lett. **89**, 078301 (2002); J. Chen, Y. Cao, and Z. Jiao, Phys. Rev. E **69**, 041403 (2004); C. Reichhardt and C.J. Olson Reichhardt, Phys. Rev. Lett. **103**, 168301 (2009).  
[2] A. Libál, C. Reichhardt, B. Jankó, and C.J. Olson Reichhardt, Phys. Rev. Lett. **96**, 188301 (2006); C. Reichhardt and C.J. Olson Reichhardt, Phys. Rev. E **79**, 061403 (2009).